SLAC–PUB–16827

Polarization Control in an X-Ray Free-Electron Laser

Alberto A. Lutman[1†], James P. MacArthur[1], Markus Ilchen[1,2,3], Anton O. Lindahl[3,4], Jens Buck[2], Ryan N. Coffee[1,3], Georgi L. Dakovski[1], Lars Dammann[5], Yuantao Ding[1], Hermann A. Dürr[1,3,6], Leif Glaser[5], Jan Grünert[2], Gregor Hartmann[5], Nick Hartmann[1,7], Daniel Higley[1], Konstantin Hirsch[1], Yurii I. Levashov[1], Agostino Marinelli[1], Tim Maxwell[1], Ankush Mitra[1], Stefan Moeller[1], Timur Osipov[1], Franz Peters[1], Marc Planas[2], Ivan Schevchuk[5], William F. Schlotter[1], Frank Scholz[5], Jörn Seltmann[5], Jens Viefhaus[5], Peter Walter[5], Zachary R. Wolf[1], Zhirong Huang[1,3], Heinz-Dieter Nuhn[1]

[1] SLAC National Accelerator Laboratory, Menlo Park, CA 94025, USA, [2] European XFEL GmbH, Hamburg 22761, Germany, [3] Stanford PULSE Institute, SLAC, Menlo Park, CA 94025, USA, [4] Department of Physics, University of Gothenburg, Sweden, [5] Deutsches Elektronen-Synchrotron DESY, Hamburg 22607, Germany, [6] Stanford Institute for Materials and Energy Sciences (SIMES), SLAC, Menlo Park, CA 94025, USA, [7] Institute of Applied Physics, University of Bern, 3012 Bern, Switzerland

Abstract

X-ray Free-Electron Lasers (XFELs) are unique sources of high brightness coherent radiation. However, existing XFELs supply only linearly polarized light, precluding studies of chiral dynamics. A device called the Delta undulator has been installed at the Linac Coherent Light Source (LCLS) to provide tunable polarization. With a reverse tapered planar undulator line to pre-microbunch the beam and the novel technique of beam diverting, hundreds of microjoules of circularly polarized X-ray pulses are produced at 500-1200 eV. These X-ray pulses are tens of femtoseconds long, have a degree of circular polarization of $0.98^{+0.02}_{-0.04}$ at 707 eV, and may be scanned in energy. We also present a new two-color X-ray pump X-ray probe operating mode for LCLS. Energy differences of $\Delta E/E = 2.4\%$ are supported, and the second pulse can be adjusted to any elliptical polarization. In this mode the pointing, timing, intensity, and wavelength of the two pulses can be modified.

Nature Photonics ***10****, 468-472 (2016), doi:10.1038/nphoton.2016.79*

Work supported by Department of Energy contract DE-AC02-76SF00515.

† aal@slac.stanford.edu

This material is based upon work supported by the U.S. Department of Energy, Office of Science, under Contract No. DE-AC02-76SF00515.

INTRODUCTION

Circularly polarized light is a powerful tool for probing electronic spin, with a special significance for studies of magnetic materials [1] and biologically important molecular systems with a handedness [2]. Research in these areas includes novel designs for spin control toward all-optical data storage [3], the control of chiral pharmaceuticals [4], and efforts to understand the origin of the homochirality of life [5]. While a range of photon energies are used to answer these questions, high photoexcitation cross sections and the ability to probe on a small spatial scale make X-rays particularly important.

Exploring the time evolution of a chiral restructuring process, be it the dissociation of a molecule or spin dynamics in a magnetized film [6], is an active field of inquiry. Chemical reactions and ultrafast magnetic switching are usually started by optical laser pulses with durations of hundreds down to fractions of a femtosecond. X-ray pump pulses have been used as an element specific trigger of non-linear dynamics [7]. Precisely timed femtosecond pulses can be used to probe the ensuing dynamics. X-rays offer the distinct advantage of elemental and orbital sensitivity as their energy can be tuned to core-valence resonances. X-ray Magnetic Circular Dichroism (XMCD) at the 2p-3d L-edges of transition metals and 3d-4f M-edges of rare earth ions has been an extremely successful tool to probe magnetic properties at synchrotron light sources in the soft X-ray photon energy range [8].

To satisfy these experimental needs various insertion devices have been used [9]. Off bending-plane synchrotron radiation [10] and elliptically polarized undulator radiation [11] supply wavelength tunable circularly polarized X-rays. However, synchrotron radiation from storage rings is limited to picosecond pulse durations and provides insufficient intensity to record snapshots of ultrafast chemical or physical processes. Excellent time resolution may be easily achieved with conventional lasers and high harmonic generation (HHG) sources, but HHG sources cannot reach X-ray wavelengths without a significant decrease in intensity [12, 13]. Storage ring based Free-Electron Lasers (FEL) [14] can generate beams at UV and VUV wavelengths with polarization control. The linac-based FERMI FEL in Italy [15] has produced circularly polarized beams reaching photon energies as high as 290 eV using a two-stage high-gain harmonic generation scheme [16], but the single pulse intensity drops to ≈ 10 μJ [17]. Finally, magnetized films have polarized soft X-ray beams at specific energies at the cost of several orders of magnitude in intensity and a degree of circular polarization

below 60% [18, 19].

Here we extend polarization control at FELs to the X-rays using the Linac Coherent Light Source (LCLS) [20]. Variable polarization has been enabled by the recently installed Delta undulator [21] built at SLAC National Accelerator Laboratory and based on a prototype device demonstrated at Cornell [22]. To achieve the highest degree of circular polarization and stability, we combine the first use of a reverse tapered undulator to suppress background power [23] with the novel technique of beam diverting. We also demonstrate a new scheme for variable polarization X-ray pump X-ray probe experiments. This scheme is capable of generating two different color pulses with control over the color separation, delay between the pulses, second pulse polarization, and pointing.

MACHINE LAYOUT

The LCLS is an X-ray free-electron laser based on planar, permanent magnet undulators. These undulators produce horizontally polarized X-rays between 270 eV and 12.8 keV.

Each undulator segment has a magnetic length of 3.3 m and a period of 3 cm. A canted pole design allows for the adjustment of the magnetic strength parameter, K, between 3.44 and 3.51. The FEL radiation wavelength λ_r depends on the undulator period λ_u and the electron beam Lorentz factor γ,

$$\lambda_r = \lambda_u \frac{1 + K^2/2 + \gamma^2\phi^2}{2\gamma^2}, \tag{1}$$

where ϕ is observation angle from the undulator axis.

K is typically decreased along the undulator line to compensate for radiative and wake-field energy loss in the electron beam. A post-saturation taper is often applied to extract additional power from the electron beam [24]. A single electron bunch may also generate two different wavelength pulses by passing through undulator sections tuned to different K values [25, 26].

There are three undulator sections separated by magnetic chicanes. These sections are 8, 6 and 16 undulator segments long. Magnetic chicanes were introduced in the undulator line to enable soft X-ray [27] and hard X-ray self-seeding [28, 29] schemes. The soft X-ray chicane, located after the eighth undulator, can delay the electrons up to 900 fs for energies up to 1.2 keV, with a designed accuracy of 0.5 fs. Above 1.2 keV the delay is limited by

the maximum magnet strength and depends on the electron beam energy. The hard X-ray chicane, located after the fourteenth undulator, can delay the electrons up to 50 fs, with an accuracy of 0.2% of the nominal delay set. A permanent magnet phase shifter and the Delta are downstream from the final planar undulator.

The Delta is a 3.2 m long variable polarization undulator with a period of 3.2 cm. It consists of four parallel longitudinal rows of $Nd_2Fe_{14}B$ magnetic blocks. The four rows form two crossed permanent magnet undulators. The degree of circular polarization, polarization angle, and undulator K value may be changed by adjusting the relative row positions along the beam direction. The maximum K strength in Delta for any elliptical polarization having the major axis either in the horizontal or the vertical direction is 3.6. This is sufficient to tune the Delta in resonance with the regular LCLS undulators.

Each undulator segment can be repointed in both horizontal and vertical directions. The electron beam can be redirected with horizontal and vertical dipole correctors between each undulator segment. This allows for the angular displacement of photon beams produced in different sections of the undulator line, a feature used in the following schemes.

A four jaw collimator using B_4C as absorbing material is located 75 m downstream of the Delta. A YAG screen 87 m downstream of the Delta can be inserted to measure the transverse profile of the photon beam.

Table I summarizes the machine conditions for the experiments presented in this Article.

CIRCULARLY POLARIZED BEAMS

The Delta can produce circularly polarized spontaneous radiation starting from the electron beam shot noise, but it is far too short to produce FEL radiation. Instead, upstream planar undulators can be used to microbunch the beam at the desired wavelength before it enters the Delta. This is commonly referred to as an afterburner configuration. The linearly polarized radiation from upstream undulators can also seed the FEL interaction in the Delta. If the Delta is in a circular polarizing mode, for example, half of the linearly polarized light will interact and be amplified in the Delta.

A variable polarizing undulator in an afterburner configuration may generate circularly polarized radiation in several ways. One technique is to generate plane polarized radiation perpendicular and 90 degrees out of phase with the radiation of the upstream planar undu-

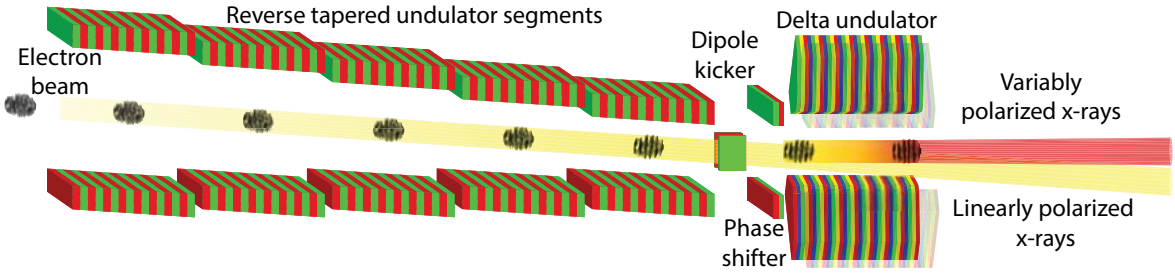

FIG. 1. **Reverse taper and beam diverting.** A relativistic electron beam is microbunched in planar undulator segments. The planar undulator gap decreases along the beam direction. This reverse tapered undulator configuration suppresses linearly polarized radiation. A dipole kicker redirects the beam into the repointed Delta undulator. The Delta undulator produces arbitrarily polarized X-rays. A phase shifter gives control over the phase between the linearly polarized FEL light at the entrance of the Delta and the microbunches in the electron beam.

lators. This crossed undulator [30–32] scheme suffers from variable polarization along the beam due to the stochastic nature of SASE spike growth in the time domain[33] and the slippage between polarization components. Non-uniform longitudinal electron beam characteristics like current, energy spread, and emittance exacerbate this problem. A related scheme involves a relatively weak plane polarized seed and an afterburner configured in an elliptical polarization. If the afterburner is set to the right relative phase and ellipticity, the final beam may be highly circularly polarized. This scheme still suffers from variable polarization along the beam. The stochastic polarization variability and the slippage between polarization components become less critical when the power ratio before and after the afterburner is higher. The power ratio in afterburner mode depends on the FEL gain length[24]. A power ratio of 5 is typical for LCLS operating at 700 eV as specified in the Single-color configuration of Table I.

In order to increase the power contrast, a reverse tapered planar undulator line has been suggested [23]. In a reverse taper K is increased along the undulator segments. This suppresses FEL radiation, but allows for strong microbunching growth (see Fig. 1). The reverse taper also decreases the FEL radiation divergence as compared with a regular taper configuration.

The degree of circular polarization can be maximized by scanning the ellipticity of the Delta as in the afterburner mode. Experimentally, the optimization was performed by

minimizing the degree of linear polarization measured by an angle resolving photoelectron Time-Of-Flight (TOF) spectrometer [34]. The spectrometer consists of 16 TOFs aligned perpendicular to the beam propagation direction. In this case, the TOFs recorded angle-dependent spectra of electrons ionized from the O 1s orbital of molecular oxygen. Due to spherical symmetry of the 1s orbital, photoelectrons are emitted along the polarization axis. Thus, circularly polarized light produces an isotropic emission pattern. In addition to these online measurements, unambiguous proof of a high degree of circular polarization was demonstrated by circular dichroism measurements in the photoemission from oriented electronic states of molecular oxygen [35].

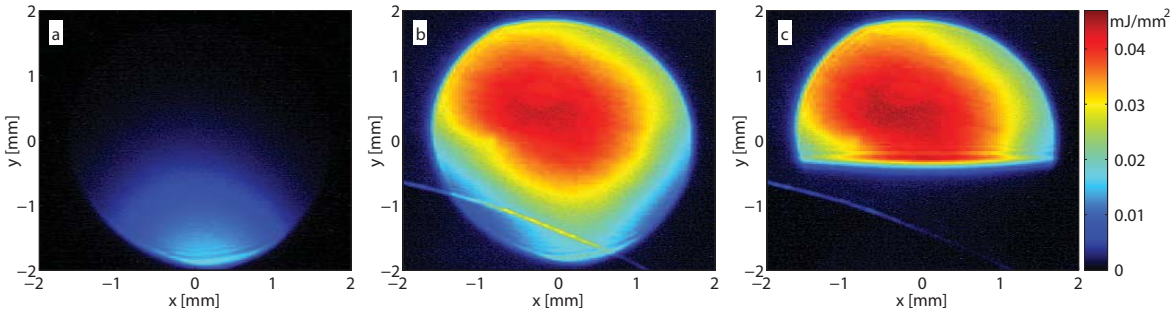

FIG. 2. **X-ray profiles in the diverted beam scheme.** Single-shot, 707 eV X-ray profiles measured at the YAG screen located 87 m downstream from the Delta. (**a**) A 19 μJ photon beam generated from a reverse tapered planar undulator line pointed down. Delta is off. (**b**) A 304 μJ photon beam measured by setting the Delta on resonance in circular polarization mode. The beam diverting scheme directs the circular light upwards. (**c**) A 205 μJ photon beam measured after inserting the collimator to block the linearly polarized light. The YAG crystal on (**b**) and (**c**) is partially saturated and the artifact is a crack on the YAG crystal.

Typical performance using the reverse taper scheme under the single color beam conditions of Table I are an average total intensity of 350 μJ with a 20 ± 12 μJ linearly polarized background from the planar undulators.

To further improve the degree of polarization and the polarization stability, a diverted beam scheme has been developed. In this scheme the circularly polarized beam from the Delta and the linearly polarized beam from the upstream undulators propagate in slightly different directions. To accomplish this, the undulator beamline preceding the Delta is re-pointed off the machine axis and the electron beam is kicked to follow the re-pointed

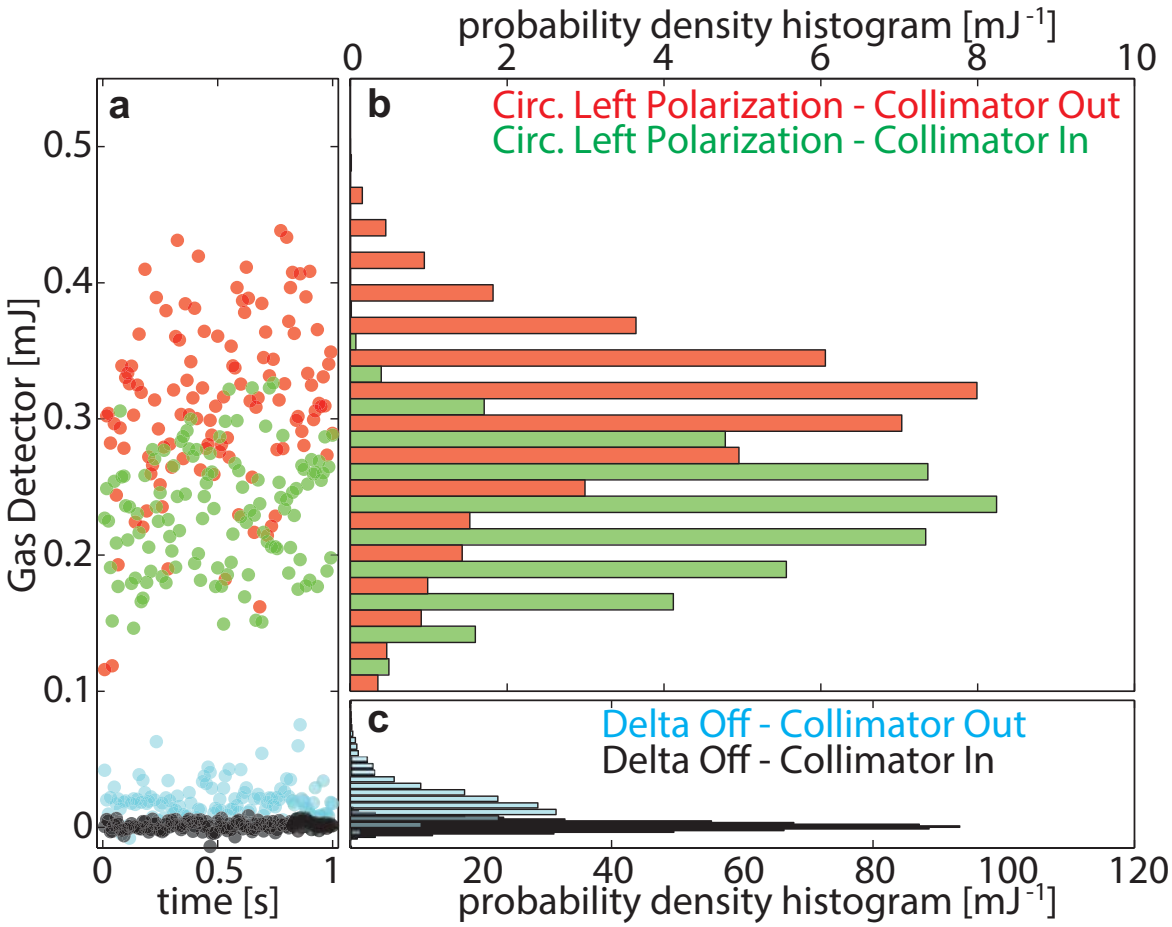

FIG. 3. **Circular polarization performance at 707 eV.** (**a**) One second of X-ray intensities as measured by the gas detector in four different conditions. (**b-c**) Intensity histograms from 3000 consecutive gas detector readings. The linearly polarized light intensity scatter (blue) is eliminated when the collimator is used (black).

direction. The linearly polarized photon beam pointing follows suit. The dipole corrector in front of the Delta is then used to give a kick to the electron beam in the desired circularly polarized photon beam direction (see Fig. 1). The K value of the Delta is also decreased so that the resonance condition (1) is still satisfied. The gain in Delta is lower at large angles, but it is not severely degraded in these parameter regimes. The optimal angle is therefore chosen in a way to have spatially fully separated beams, without sacrificing much intensity.

The diverted beam scheme is used together with a reverse taper. The reverse taper supplies a low intensity, small divergence linearly polarized beam. This makes it easier to

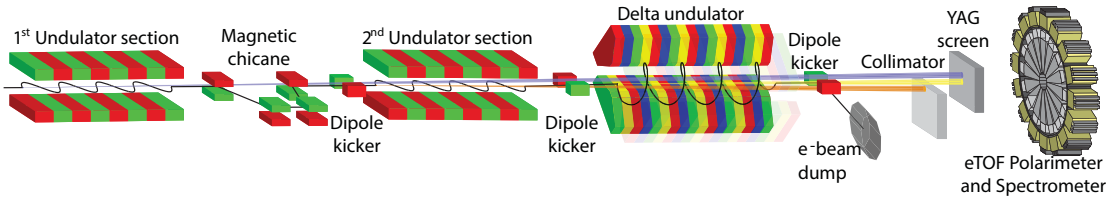

FIG. 4. **Two-Color Two-Polarization scheme**. In the first undulator section a SASE photon pulse is generated at the energy E_1 by tuning the undulator to K_1. The magnetic chicane delays the electrons with respect to the photon beam. In the second undulator section, tuned to K_2, the electron beam develops microbunching at wavelength λ_2 lasing at energy E_2, and a second linearly polarized beam is generated. The Delta is tuned on resonance at λ_2 at the desired polarization generating the second pulse with polarization control. The diverted beam scheme is applied and the linearly polarized beam at E_2 is stopped by the collimator. LCLS undulator beamline sections can be re-pointed independently, and either overlap or transverse separation between the beams can be provided. A YAG screen is used as transverse diagnostic. Spectrum and polarization are resolved by the eTOF polarimeter and spectrometer.

TABLE I. Experimental machine conditions.

	Single-color	Two-color
Electron energy	4 GeV	4.5 GeV
Photon energy	707 eV	930 eV
Bunch charge	167 pC	150 pC
Beam core current	4.3 kA	1.5 kA
1^{st} color und. segments	6 Regular and Delta	8 Regular
2^{nd} color und. segments	n/a	7 Regular and Delta

block the background linearly polarized beam.

Figure 2 shows measured single-shot transverse profiles of the photon beams on the YAG detector. Panel 2**a** shows the photon beam with the Delta set to the off configuration; only the linearly polarized beam pointing downwards is visible. Panel 2**b** shows the full beam with Delta set on resonance with an angular separation of ~ 30 μrad from the linearly polarized one, typical around 700 eV. Panel 2**c** shows a transverse profile with the collimator

TABLE II. Intensity performance for the Delta undulator operating in both circular polarization modes with the diverted beam configuration. Each dataset consists of 3000 consecutive shots.

Condition	Beam energy [μJ][a]
Delta off, Collimator out	19 ± 13
Delta off, Collimator in	1.1 ± 3.5 [b]
Delta on, Circular Left, Collimator out	298 ± 70
Delta on, Circular Left, Collimator in	225 ± 49
Delta on, Circular Right, Collimator out	345 ± 67
Delta on, Circular Right, Collimator in	208 ± 45

[a] Confidence interval expressed as average plus/minus single standard deviation.

[b] Standard deviation of the detector with the collimator fully inserted was measured to be 2 μJ.

jaw inserted in the photon beam path to block the linearly polarized light.

The collimator jaw does obstruct a portion of the light generated by the Delta, but it almost completely eliminates power fluctuations in the background linearly polarized light. Figure 3 shows this decrease in background fluctuations by plotting gas detector intensities with the collimator inserted (black) and with the collimator out (blue). This decrease in background fluctuations improves the polarization stability. The collimator does block 25% of the circular light from Delta, as seen by comparing the green and red histograms.

The diverted beam scheme allows for the maximum degree of circular polarization and stability. This scheme was successfully used for recording XMCD spectra across the iron L_2 and L_3 edges of thin film GdFeCo samples, as well as following the dynamic XMCD signal at the iron L_3 (707 eV) and gadolinium M_5 (1190 eV) edges as a function of delay after optical pump excitation [36]. The degree of circular polarization was measured at 707 eV to be $0.98^{+0.02}_{-0.04}$ by comparing the magnitude of the XMCD signal integrated over the iron L_3 edge of a 40 nm GdFeCo sample to that at a source with a known degree of polarization, beamline 4.0.2 at the Advanced Light Source. The capability of performing fast photon energy scans by changing the electron beam energy and the capability of switching the photon beam chirality were also demonstrated during the experiment.

Table II summarizes the experimental performance achieved during that experiment performed in the Single-color machine conditions summarized in Table I. A reverse tapered

configuration was set for the six undulator segments used to microbunch the electron beam. XTCAV analysis [37] revealed that only 58% of the charge was contributing to the lasing process. The lasing electron beam core had a peak current of 4.3 kA and a duration of 23 fs. Switching between left and right circular polarization was done in 35 seconds, the time required by the Delta rows to switch between the two resonant configurations. During the experiment, scans were performed in a 30 eV range to cover the L_2 and L_3 iron edges at 720 and 707 eV.

TWO-COLOR TWO-POLARIZATION BEAMS

The addition of the Delta to the LCLS undulator line allows for a new two-color, two-polarization operation mode. A schematic is shown in Figure 4. The first undulator section tuned at a strength K_1 is used to generate a horizontally polarized photon beam at energy E_1. A magnetic chicane can be used to delay the electron beam with respect to the generated photon beam, granting control on the temporal delay between the first photon beam and the photon beams generated downstream of the chicane.

The second undulator section and the Delta are tuned as previously described to generate a circularly polarized beam. A different undulator strength K_2 can be used for the second undulator section. The best results are obtained with a reverse tapered undulator and beam diverting. This yields two additional beams, one linearly polarized and one circularly polarized.

The beams at E_2 are temporally almost coincident. The photon beam at E_1 precedes the other beams by at least the intrinsic delay. The intrinsic delay, usually on the order of few femtoseconds, can be estimated from the radiation wavelength and the undulator configuration[25]. The temporal delay between the beams can only be increased by means of the magnetic chicanes. If the first 8 undulator segments are sufficient to generate the first color, both chicanes can be used. This allows a delay of up to 950 fs for energies below 1.2 keV. Otherwise, the hard X-ray chicane can generate a 50 fs maximum delay.

Experimental conditions for two-color variable polarization scheme are listed in the second column of Table I. The chicane was left off yielding near temporal overlap between the beams and the diverted beam scheme was applied in the second section. The photon energy separation was 15 eV. The first undulator section was repointed to ensure transverse overlap

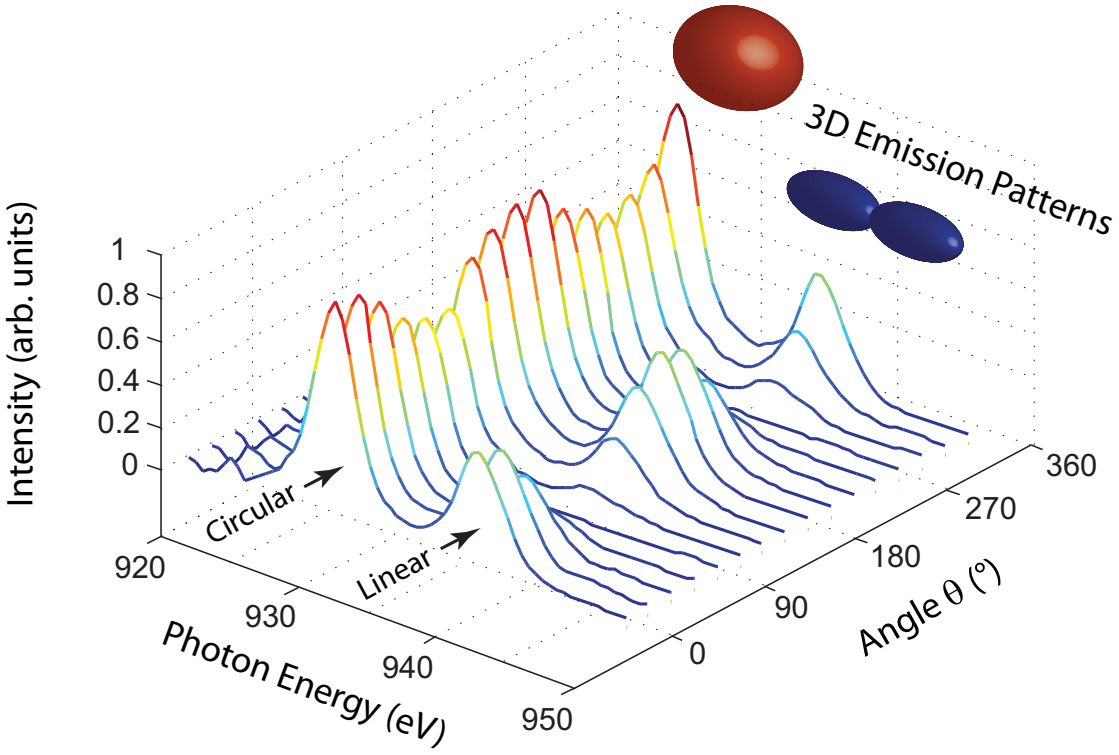

FIG. 5. **Two-Color Two-Polarization experimental demonstration.** Photon energy average spectra from 16 spectrometers aligned in the plane of the polarization vectors. The patterns follow a Legendre polynomial of second order which has been used to derive the degrees of linear and circular polarization. The insets above the spectra display the derived 3D emission patterns of Ne 1s photoelectrons in both polarization modes.

between the linearly polarized beam at the first photon energy and the circularly polarized photon beam.

The mean photon beam intensity was measured with the gas detector to be 34 μJ, with the circular polarized beam four times more intense than the linearly polarized one. The low total pulse intensity is a result of a low electron peak current. The low peak current increases the gain length, decreasing the amount of light that can be produced in a single undulator segment. The electron beam energy spread growth during the first lasing process also degrades performance in the second lasing process.

The spectral and polarization properties of the two-color two-polarization experiment

were assessed with the TOF polarimeter described previously. Atomic neon ($E_{\mathrm{bind}} = 870\,\mathrm{eV}$) was used as a target. Figure 5 shows all 16 spectral traces for the Ne 1s photoelectrons after time-to-energy conversion. The two different colors have substantially different angular emission patterns. A fit to this distribution shows that the higher energy photon beam has a degree of linear polarization of $1.00^{+0.00}_{-0.01}$. With the assumption that the lower energy photon beam has no unpolarized component, it has an average degree of circular polarization of 0.97 $\pm$0.03.

DISCUSSION

We demonstrated the first variable polarization X-ray FEL reaching energies well above 290 eV, by the addition of the Delta at the LCLS. 200 μJ X-ray pulses were produced with a nearly pure circular polarization. Circularly polarized beams have already been used in two experiments [35, 36].

The highest degree of circular polarization was achieved by applying two new techniques. A reverse taper was used to suppress background FEL radiation, and the beam diversion technique proposed and demonstrated here was used to spatially separate polarization components. Spatial separation ensures that photons that are not blocked are generated almost exclusively in the Delta. This grants polarization control by setting the polarization state of the Delta and allows tuning on photon beam intensities rather than on online polarization measurements requiring dedicated instruments.

We demonstrated a two-color two-polarization scheme, where a linearly polarized X-ray pulse at one color is followed by a pulse with circular polarization at a second color. The delay between the pulses can be controlled by adjusting an electron beam chicane delay. The photon beam was resolved in both spectrum and polarization by an angle resolving photoelectron Time-Of-Flight spectrometer.

Multi-color operation with up to four photon beams may be possible by combining the techniques presented in this article with twin-bunch operation [38]. In this case, two beams would be linearly polarized and two beams circularly polarized, with two to four different wavelengths.

Finally the diverted beam scheme could be used to spatially separate any two pulses generated in different undulator segments. A relevant application would be separating the

wide-bandwidth pre-pulse present in the hard X-ray self-seeding schemes based on a crystal monochromator [28, 29] from the desired narrow-bandwidth pulse.

CONTRIBUTION STATEMENT

A.A.L., J.P.M., M.I., A.O.L., Z.H. and H.-D.N. co-wrote the manuscript. A.A.L. conceived of the beam diverting and two-color, two-polarization schemes. J.P.M., A.M., Y.D., and Z.H. provided modeling and theoretical support for the reverse taper and beam diverting techniques. A.A.L., J.P.M., Y.D., A.M., T.M., F.P., Z.R.W., Z.H. and H.-D.N. configured the LCLS and the Delta for photon beam generation during the experiments. M.I., A.O.L., J.B., R.N.C., L.D., L.G., J.G., G.H., N.H., S.M., A.M, T.O., M.P., I.S., F.S., J.S., J.V. and P.W. prepared the online diagnostic experiments with the e-TOF polarimeter.. M.I., A.O.L., J.B., R.N.C., L.D., J.G.,G.H.,N.H.,S.M.,T.O.,M.P.,F.S.,I.S.,J.S.,J.V., and P.W. performed the experiments with the e-TOF polarimeter, with A.O.L., M.I., G.H. and J.B. analyzing the data offline. A.O.L. provided the online data analysis. D.H., G.L.D., H.A.D., K.H. and W.F.S. measured the photon beam with the XMCD technique, with D.H. and K.H. analyzing the data. F.P. designed the Delta built at SLAC. Z.R.W. and Y.I.L. measured and tuned the Delta before installation. H.-D.N. is the Delta undulator project lead.

ACKNOWLEDGMENTS

We are thankful for the support of C.P. O'Grady for the online data handling system. This work was supported by DOE Contract No. DE-AC02-76SF00515.
A.O.L. acknowledges funding from the Knut and Alice Wallenberg foundation through the Max IV synchrotron radiation facility program.

COMPETING FINANCIAL INTERESTS STATEMENT

The authors have no significant competing financial, professional or personal interests that might have influenced the performance or presentation of the work described in this manuscript.

* aal@slac.stanford.edu

[1] Schütz, G. *et al.* Absorption of circularly polarized x rays in iron. *Phys. Rev. Lett.* **58**, 737–740 (1987).

[2] Hergenhahn, U. *et al.* Photoelectron circular dichroism in core level ionization of randomly oriented pure enantiomers of the chiral molecule camphor. *The Journal of Chemical Physics* **120**, 4553–4556 (2004).

[3] Graves, C., Reid, A. H. *et al.* Nanoscale spin reversal by non-local angular momentum transfer following ultrafast laser excitation in ferrimagnetic gdfeco. *Nat. Materials* **12**, 293–298 (2013).

[4] Nguyen, L. A., He, H. & Pham-Huy, C. Chiral drugs: an overview. *Int J Biomed Sci* **2**, 85–100 (2006).

[5] Böwering, N. *et al.* Asymmetry in photoelectron emission from chiral molecules induced by circularly polarized light. *Phys. Rev. Lett.* **86**, 1187–1190 (2001).

[6] von Korff Schmising, C. *et al.* Imaging ultrafast demagnetization dynamics after a spatially localized optical excitation. *Phys. Rev. Lett.* **112**, 217203 (2014).

[7] Rohringer, N. *et al.* Atomic inner-shell x-ray laser at 1.46 nanometres pumped by an x-ray free-electron laser. *Nature* **481**, 488–491 (2012).

[8] Stöhr, J. & Siegmann, H. *Magnetism: From Fundamentals to Nanoscale Dynamics*. Springer Series in Solid-State Sciences (Springer Berlin Heidelberg, 2006).

[9] Elleaume, P. Generation of various polarization states from insertion devices: A review. *Review of Scientific Instruments* **60**, 1830–1833 (1989).

[10] Chen, C. T., Sette, F., Ma, Y. & Modesti, S. Soft-x-ray magnetic circular dichroism at the $l_{2,3}$ edges of nickel. *Phys. Rev. B* **42**, 7262–7265 (1990).

[11] Sasaki, S., Shimada, T., ichi Yanagida, K., Kobayashi, H. & Miyahara, Y. First observation of undulator radiation from apple-1. *Nuclear Instruments and Methods in Physics Research Section A: Accelerators, Spectrometers, Detectors and Associated Equipment* **347**, 87 – 91 (1994).

[12] Popmintchev, T. *et al.* Bright coherent ultrahigh harmonics in the kev x-ray regime from mid-infrared femtosecond lasers. *Science* **336**, 1287–1291 (2012).

[13] Vodungbo, B. *et al.* Polarization control of high order harmonics in the euv photon energy range. *Opt. Express* **19**, 4346–4356 (2011).

[14] Litvinenko, V. N. *et al.* The OK-5/Duke storage ring VUV FEL with variable polarization. *Nuclear Instruments and Methods in Physics Research A* **475**, 407–416 (2001).

[15] Allaria, E. *et al.* Highly coherent and stable pulses from the fermi seeded free-electron laser in the extreme ultraviolet. *Nat. Photon.* **6**, 699–704 (2012).

[16] Allaria, E. *et al.* Two-stage seeded soft-x-ray free-electron laser. *Nat. Photon.* **7**, 913–918 (2013).

[17] Allaria, E. *et al.* The FERMI free-electron lasers. *Journal of Synchrotron Radiation* **22**, 485–491 (2015).

[18] Pfau, B. *et al.* Magnetic imaging at linearly polarized x-ray sources. *Opt. Express* **18**, 13608–13615 (2010).

[19] Wang, T. *et al.* Femtosecond single-shot imaging of nanoscale ferromagnetic order in Co/Pd multilayers using resonant x-ray holography. *Phys. Rev. Lett.* **108**, 267403 (2012).

[20] Emma, P. *et al.* First lasing and operation of an angstrom-wavelength free-electron laser. *Nat. Photon.* **4**, 641–647 (2009).

[21] Nuhn, H.-D. *et al.* R&D towards a delta-type undulator for the LCLS. In *Proceedings, 35th International Free Electron Laser Conference (FEL2013)*, 348–350 (New York, NY, USA, 2013).

[22] Temnykh, A. B. Delta undulator for cornell energy recovery linac. *Phys. Rev. ST Accel. Beams* **11**, 120702 (2008).

[23] Schneidmiller, E. A. & Yurkov, M. V. Obtaining high degree of circular polarization at x-ray free electron lasers via a reverse undulator taper. *Phys. Rev. ST Accel. Beams* **16**, 110702 (2013).

[24] Huang, Z. & Kim, K.-J. Review of x-ray free-electron laser theory. *Phys. Rev. ST Accel. Beams* **10**, 034801 (2007).

[25] Lutman, A. A. *et al.* Experimental demonstration of femtosecond two-color x-ray free-electron lasers. *Phys. Rev. Lett.* **110**, 134801 (2013).

[26] Marinelli, A. *et al.* Multicolor operation and spectral control in a gain-modulated x-ray free-electron laser. *Phys. Rev. Lett.* **111**, 134801 (2013).

[27] Ratner, D. *et al.* Experimental demonstration of a soft x-ray self-seeded free-electron laser. *Phys. Rev. Lett.* **114**, 054801 (2015).

[28] Amman, J. *et al.* Demonstration of self-seeding in a hard-x-ray free-electron laser. *Nat. Photon.* **6**, 693–698 (2012).

[29] Lutman, A. A. *et al.* Demonstration of single-crystal self-seeded two-color x-ray free-electron lasers. *Phys. Rev. Lett.* **113**, 254801 (2014).

[30] Kim, K. J. A synchrotron radiation source with arbitrarily adjustable elliptical polarization. *Nuclear Instruments and Methods in Physics Research* **219**, 425 – 429 (1984).

[31] Deng, H. *et al.* Polarization switching demonstration using crossed-planar undulators in a seeded free-electron laser. *Phys. Rev. ST Accel. Beams* **17**, 020704 (2014).

[32] Ferrari, E. *et al.* Single shot polarization characterization of xuv fel pulses from crossed polarized undulators. *Scientific Reports* **5** (2015).

[33] Ding, Y. & Huang, Z. Statistical analysis of crossed undulator for polarization control in a self-amplified spontaneous emission free electron laser. *Phys. Rev. ST Accel. Beams* **11**, 030702 (2008).

[34] Allaria, E. *et al.* Control of the polarization of a vacuum-ultraviolet, high-gain, free-electron laser. *Phys. Rev. X* **4**, 041040 (2014).

[35] Hartmann, G. *et al.* Circular dichroism measurement at an x-ray free-electron laser with polarization control. *under review APL* **n/a**, n/a (2015).

[36] Higley, D. J. *et al.* Femtosecond X-ray magnetic circular dichroism absorption spectroscopy at an X-ray free electron laser. *ArXiv e-prints* (2015). arXiv:1511.07372.

[37] Behrens, C. *et al.* Few-femtosecond time-resolved measurements of x-ray free-electron lasers. *Nature Communications* **5** 3762 (2014).

[38] Marinelli, A. *et al.* High-intensity double-pulse x-ray free-electron laser. *Nature Communications* **6**, 6369 (2015).